ELSEVIER

Polymer 43 (2002) 6323–6331

polymer

www.elsevier.com/locate/polymer

Electronic momentum distribution in the one-dimensional extended Hubbard model: determinantal Monte Carlo study

S. Goumri-Said[a,b,*], H. Aourag[a,c], L. Salomon[b,c], J.-P. Dufour[b]

[a]*Computational Materials Science Laboratory, Department of Physics, University of Sidi Bel-Abbes, 22 Rue Hoche, Sidi Bel-Abbes 22000, Algeria*
[b]*Laboratoire de Physique, Groupe d'Optique de Champ Proche, Faculté des Sciences Mirande, CNRS UMR 5027, Université de Bourgogne, 9 Avenue Alain Savary, BP 47 870-21078 Dijon Cedex, France*
[c]*LERMPS, Université de Technologie de Belfort-Montbeliard, Site des Sévenans, 90010, Belfort, France*

Received 2 March 2002; received in revised form 29 July 2002; accepted 30 July 2002

Abstract

The effect of electron–electron (e–e) interaction on *trans*-polyacetylene (*t*-PA) properties is investigated within the framework of an extended Hubbard model in one dimension. For numerical calculation, we use the determinantal version of quantum Monte Carlo approach, which provides a breakthrough to simulate statistical fluctuations in the systems with many degrees of freedom, in order to obtain mean values for observables of physical interest. This allows one to analyze the discrete system of fermions without encountering the numerical instabilities that generally occur from the original problem involving anticommuting fermion operators. We calculate the electronic momentum distribution function $n(k)$ for on-site interaction U and nearest-neighbor interaction E, where $U < 4t$, $U \simeq 4t$ and $U > 4t$, with $E \in [U/2, U]$, (t is the hopping matrix elements). © 2002 Published by Elsevier Science Ltd.

Keywords: Momentum distribution; Extended one-dimensional Hubbard model; Quantum Monte Carlo simulation

1. Introduction

The understanding of the electrons correlations is one of the most challenging problem in condensed matter at present. Electrons correlations in conjugated polymers have been paid a great deal of attention for the past few years following the experimental and theoretical achievements. In quasi-one-dimensional organic systems and, particularly, the advent of high temperature superconductivity has motivated renewed interest in the Hubbard model [1,2].

In theoretical field for the recent past years, there has been enormous research in both quantum chemistry and solid state physics, such as semi-empirical methods of quantum chemistry including the Pariser–Parr–Pople (PPP) model, the extended Huckel model, the complete neglect of differential overlap model, which have described quite precisely a wide range of excited state properties (linear and two-photon absorption, non-linear optical states, excited state geometries and soliton structures) in π-conjugated systems [3].

In solid state physics, the Hubbard model was introduced as a simple effective model for the study of correlation effects of d-electrons in transition metals [4]. It is believed to provide a qualitative description of the magnetic properties of these materials and of the Mott metal insulator transition. Despite of its appealing conceptual simplicity rigorous results for the Hubbard model are rare. The most explicit results have been obtained for the one-dimensional case. This is the only case where the spectrum and a complete set of eigen functions are known [5]. We should also point out that despite the existence of the Lieb-Wu [6] exact solution to the one-dimensional Hubbard model, correlation functions are known in relatively few cases. In particular, the momentum distribution, to our knowledge, has been derived from the Lieb-Wu result only at half filling and in the limit of strong on-site repulsion [7].

Our aim in this work is to determine the qualitative effect of e–e interaction on the ground state properties by determining the electronic momentum distribution observable for half filling band case. We use the better-tested determinantal quantum Monte Carlo (QMC) method based

* Corresponding author. Fax: +33-3-80-39-60-50.
E-mail address: sgoumri@u-bourgogne.fr (S. Goumri-Said).

0032-3861/02/$ - see front matter © 2002 Published by Elsevier Science Ltd.
PII: S0032-3861(02)00535-9

on the Blakenbecler, Scalapino, Sugar and Hirsch (BSSH) algorithm [8,9]. In one dimension, this algorithm is not efficient as World-line methods [10], but it is more easily generalizable to higher dimension. Also, the BSSH algorithm is designed for the grand-canonical ensemble, whose convergence to the infinite-size limit is presumably different, and perhaps even faster, than the canonical ensemble.

In Section 2, we discuss the scheme of our analysis: we discuss the extended Hubbard model and the simulation method and we implement the model to *t*-PA system. In Section 3, we give the details of our results. The present work is summarized in Section 4.

2. Model formulation and numerical work

2.1. MODEL: the extended one-dimensional Hubbard model

In this paper we shall concentrate on the extended version of one-dimensional Hubbard model. While the analytic approaches usually define the model by specifying the couplings in momentum space, for numerical approaches it is more convenient to define the model in real space. In addition, the interaction parameters in real space have a more direct interpretation in terms of overlap matrix elements of molecular orbitals in a tight-binding picture. The simplest model defined in real space, is the extended Hubbard model with on-site interaction U and nearest-neighbor interaction E, given by the following Hamiltonian [1,8,11].

$$H = -t \sum_{i=1,\sigma=\uparrow\downarrow}^{N} (c_{i,\sigma}^{+} c_{i+1,\sigma} + Hc) + U \sum_{i=1}^{N} n_{i\uparrow} n_{i\downarrow} + E \sum_{i=1}^{N} n_i n_{i+1} \tag{1}$$

where the index i label the spatial sites and σ is a spin index ($\sigma = \uparrow\downarrow$), $c_{i,\sigma}^{+}(c_{i,\sigma})$ are creation (annihilation) operators, the number operator is $n_{i\sigma} = c_{i,\sigma}^{+} c_{i,\sigma}$ and $n_i = n_{i\uparrow} + n_{i\downarrow}$, t is the hopping parameter matrix, which is introduced from the Hückel theory representing the degree to which the π-orbitals on adjacent atoms in a chain overlap. The chemical potential μ is added to fix the average number $\langle n \rangle = \langle n_{i\uparrow} + n_{i\downarrow} \rangle$, we restrict ourselves to the half-filled band, $\mu = U/2$.

2.2. Method: determinantal QMC simulation

Most of the literature on the one-dimensional Hubbard model is based on the seminal 1968 paper [12] by Lieb and Wu. In this paper, the model was solved by the determinantal QMC simulation.

The partition function, using Trotter approximation [13] in separating the one-particle and two-particle terms and dividing the imaginary time interval $[0, \beta]$ into L sub-intervals of width $\Delta\tau = \beta/L$, may be written as:

$$Z = \mathrm{Tr}(\mathrm{e}^{-\beta\hat{H}}) = \mathrm{Tr} \prod_{l=1}^{L} \mathrm{e}^{-\Delta\tau\hat{H}} \approx \mathrm{Tr} \prod_{l=1}^{L} \mathrm{e}^{-\Delta\tau\hat{H}_0} \mathrm{e}^{-\Delta\tau\hat{H}_1} \tag{2}$$

To eliminate the two-body interaction term, we use the discrete Hubbard–Stratonovich transformation [14] using the identity:

$$\mathrm{Tr} \exp(-c_i^{+} A_{ij} c_j) \exp(-c_i^{+} B_{ij} c_j) = \det(1 + \mathrm{e}^{-A} \mathrm{e}^{-B}) \tag{3}$$

for arbitrary matrices A and B and taking the trace over fermions [15], one obtains:

$$Z = \mathrm{Tr}_\sigma \prod_{\alpha=\pm 1} \prod_{l=1}^{L} [1 + B_L(\alpha) B_{L-1}(L) \cdots B_1(\alpha)] \tag{4}$$

$$= \mathrm{Tr}_\sigma \det \mathrm{O}_\uparrow \det \mathrm{O}_\downarrow \tag{5}$$

where O_σ is an $NL \times NL$ matrix,

$$\mathrm{O}_\sigma = 1 + \prod_{l=1}^{L} B_l^\sigma(\alpha) \tag{6}$$

$$B_l(\alpha) = \exp[-\Delta\tau K] \exp[V^\alpha(l)] \tag{7}$$

$$K_{i,j} = \begin{cases} -t(>0) & \text{for } i,j \text{ nearest neighbor,} \\ 0 & \text{otherwise} \end{cases}$$

$$V_{ij}^{\alpha}(l) = \delta_{ij} \left[\lambda \alpha \sigma_i(l) + \Delta\tau \left(\mu - \frac{U}{2} \right) \right] \tag{8}$$

$$\lambda = \cosh^{-1} \left(\Delta\tau \frac{U}{2} \right) \tag{9}$$

To perform the Monte Carlo simulation, we can take the determinant in Eq. (5) as the Boltzmann weight. For the case of half-filled band, the product in Eq. (3) is positive for arbitrary σ configurations [16].

The heat-bath algorithm is used to perform the sum over Ising spins. Suppose, R_α is the ratio of new to old determinant for fermion spin α on flipping a given Ising spin, the flipping probability for this, is given by:

$$P = \frac{R_\uparrow R_\downarrow}{1 + R_\uparrow R_\downarrow} \tag{10}$$

R_α can be computed by using the procedure introduced by Blakenbecler, Scalapino and Sugar [10], which involves updating the Green's function exactly when a move is accepted. Therefore, measurements of statistical averages of many observables are performed.

Let us recall, at the end of this section, that in the quantum chemistry field, the resolution of the sign problem in QMC simulation has been reported in many papers. The most popular work is the paper of Soos et al. [17], where, they resolve the problem for the PPP model.

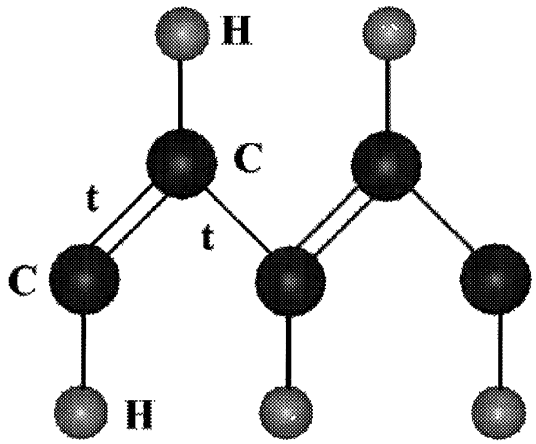

(a)

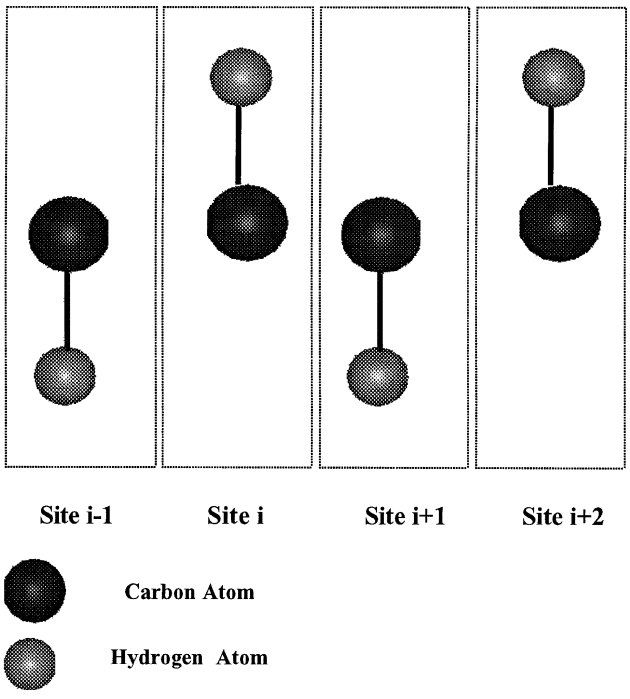

(b)

Fig. 1. (a) Schematic representation of the ground state geometry of *trans*-polyacetylene. (b) Schematic representation of the unit cell of *trans*-polyacetylene used in simulation.

3. Numerical results and discussion

The numerical study using the Monte Carlo method allows us to get quantitative and qualitative results for various statistical properties for essentially arbitrary parameters (U, E). Since the problem of convergence is delicate and depends on the physical quantity calculated as well as on the magnitude of these parameters, we are interested in an appropriate *t*-PA's set of parameters [18].

t-PA is a quasi-one-dimensional compound with a carbon backbone characterized by several types of bonds. The ground state geometry of *t*-PA is shown schematically in Fig. 1(a). The valence electronic structure is determined by the carbon 2s and 2p orbitals which, in the limit of an infinite polyene, form σ-type and π-type energy bands with the π-bands closest to the gap between the highest occupied molecular orbital (HOMO) and the lowest unoccupied molecular orbital (LUMO).

Assuming equal C–C bond lengths and a quasi-one-dimensional structure [19] this mean that the unit of repetition contains one carbon atom which contributes one electron in a $2p_z$-orbital to the π-electron system. Since there is room for two electrons in each $2p_z$-orbital this implies that the π-band is exactly half-filled. Fig. 1(b) shows the first assumption in which we take one carbon atom per unit cell. Also is shown in this figure the no-null elements of the hopping matrix having all the same absolute value *t*.

Before proceeding to the details of our results we must recall here that all the physical observables are calculated for a chain consisting of 32 sites. All that the measurements are taken only every other full Monte Carlo sweeps through the $(1 + 1)$-dimensional lattice. We have performed our calculations for the following auxiliary data: 400 warm-ups sweep and the number of time slices (L) is taken equal to 30. We must notice that this set of values is selected with a purely 'computational criterion' [9,10].

3.1. Momentum distribution

In our work, we are interested in the variation of mean values of the electronic momentum distribution $n(k)$ for all $k = k_x$; $k_x = 2\pi i_x/N_x$, $0 \preceq i_x \preceq N_x - 1$. It can be calculated in the ground state as follows:

$$n(k) = \frac{1}{2}\sum_{\sigma}\langle c^{+}_{k\sigma}c_{k\sigma}\rangle \tag{11}$$

Because the QMC calculation uses the site representation, we should perform a Fourier transformation of Eq. (11) to real space, and obtain

$$n(k) = \frac{1}{2N}\sum_{n}\sum_{l}\sum_{\sigma}\langle c^{+}_{n+1,\sigma}c_{n,\sigma}\rangle \exp(\mathrm{i}k\cdot l) \tag{12}$$

N is the site number or equivalently elementary cells.

3.1.1. Strong coupling regime: $U4t$ and $E \approx U$, $E \approx U/2$, $EU/2$, $EU/2$)

In Fig. 2(a)–(d), we represent the momentum distribution for the strong coupling regime, where $U > 10$ eV and $E \approx 5$, 7, 9 and 14 eV, respectively.

We have studied also, the effect of U and E on the behavior of $n(k)$ for fixed values of inverse temperature $\beta =$ 0.04, 0.08, 0.2, respectively, shown in Fig. 3(a)–(c). The magnitude of this observable is changing for different values of short range interaction E. This result, reflect the importance of including all range of Coulomb interaction [20].

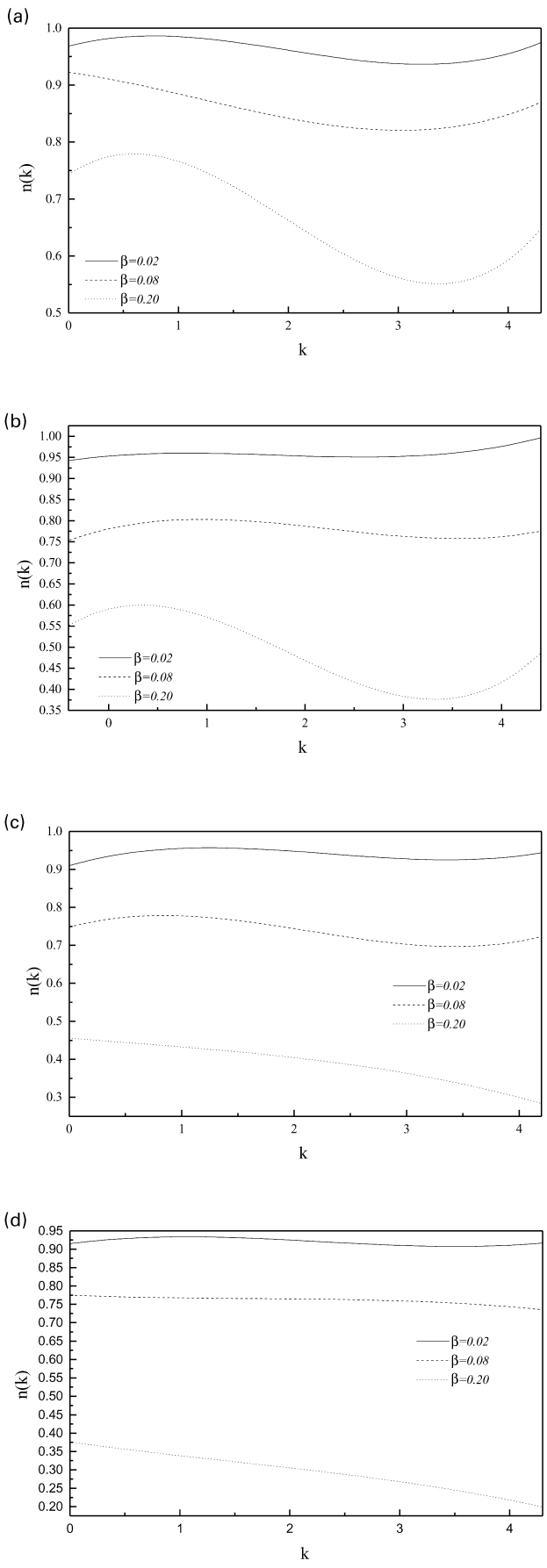

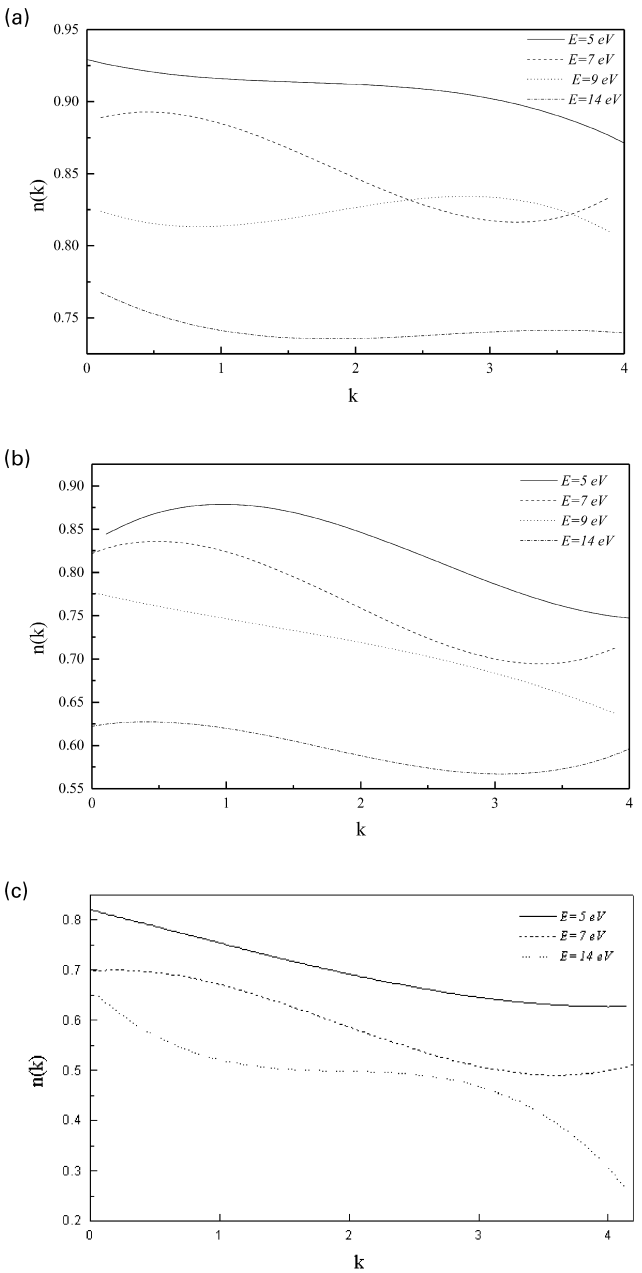

Fig. 3. (a) The variation of momentum distribution versus wave vector for ($U = 14$, $E = 5$, 7, 9, 14) (eV) and $\beta = 0.02$. (b) The variation of momentum distribution versus wave vector for ($U = 14$, $E = 5$, 7, 9, 14) (eV) and $\beta = 0.04$. (c) The variation of momentum distribution versus wave vector for ($U = 14$, $E = 5$, 7, 9, 14) (eV) and $\beta = 0.2$.

Fig. 2. (a) The variation of momentum distribution versus wave vector for different values of β ($\beta = 0.02, 0.08, 0.20$) for ($U > 10$, $E = 5$) (eV). (b) The variation of momentum distribution versus wave vector for different values of β ($\beta = 0.02, 0.08, 0.20$) for ($U > 10$, $E = 7$) (eV). (c) The variation of momentum distribution versus wave vector for different values of β ($\beta = 0.02, 0.08, 0.20$) for ($U > 10$, $E = 9$) (eV). (d) The variation of momentum distribution versus wave vector for different values of β ($\beta = 0.02, 0.08, 0.20$) for ($U > 10$, $E = 14$) (eV).

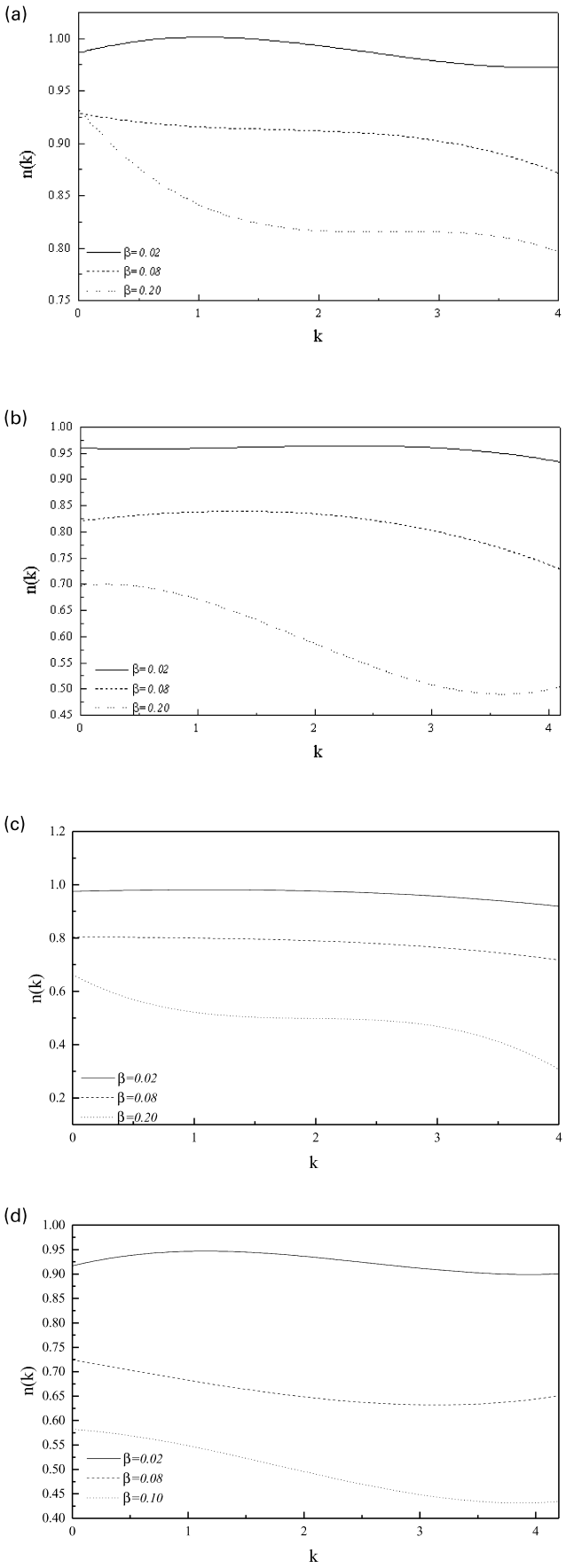

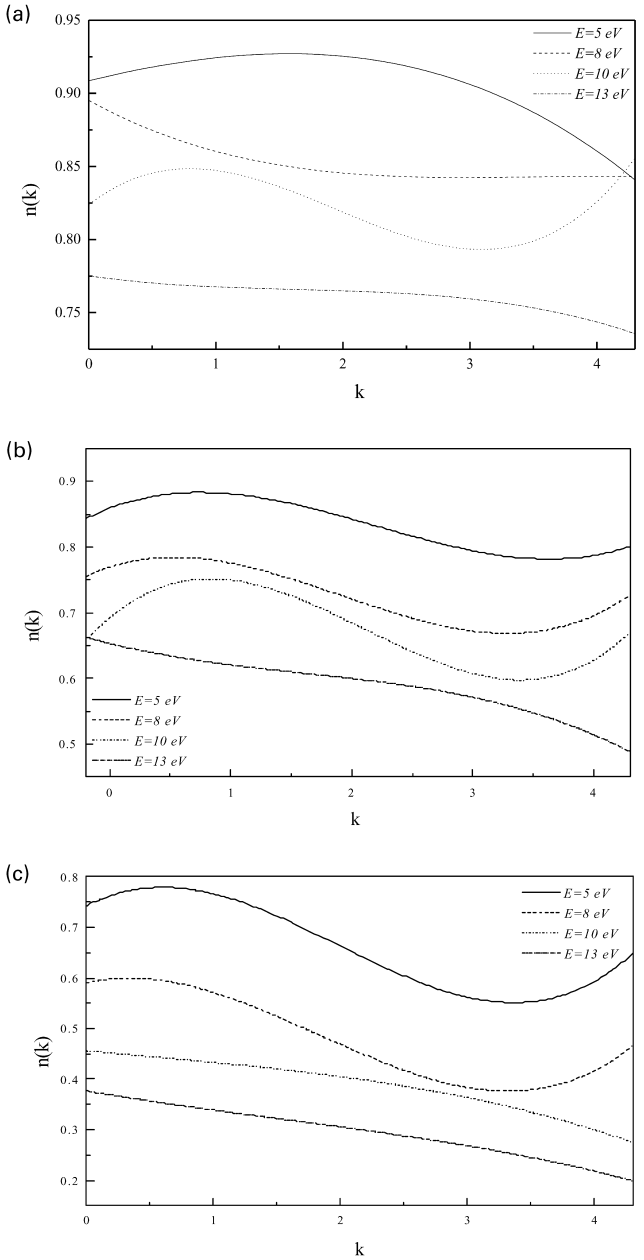

Fig. 5. (a) The variation of momentum distribution versus wave vector for ($U = 10$, $E = 5$, 8, 10, 13) (eV) and $\beta = 0.02$. (b) The variation of momentum distribution versus wave vector for ($U = 10$, $E = 5$, 8, 10, 13) (eV) and $\beta = 0.04$. (c) The variation of momentum distribution versus wave vector for ($U = 10$, $E = 5$, 8, 10, 13) (eV) and $\beta = 0.2$.

Fig. 4. (a) The variation of momentum distribution versus wave vector for different values of β ($\beta = 0.02, 0.08, 0.20$) for ($U = 10$, $E = 5$) (eV). (b) The variation of momentum distribution versus wave vector for different values of β ($\beta = 0.02, 0.08, 0.20$) for ($U = 10$, $E = 8$) (eV). (c) The variation of momentum distribution versus wave vector for different values of β ($\beta = 0.02, 0.08, 0.20$) for ($U = 10$, $E = 10$) (eV). (d) The variation of momentum distribution versus wave vector for different values of β ($\beta = 0.02, 0.08, 0.20$) for ($U = 10$, $E = 13$) (eV).

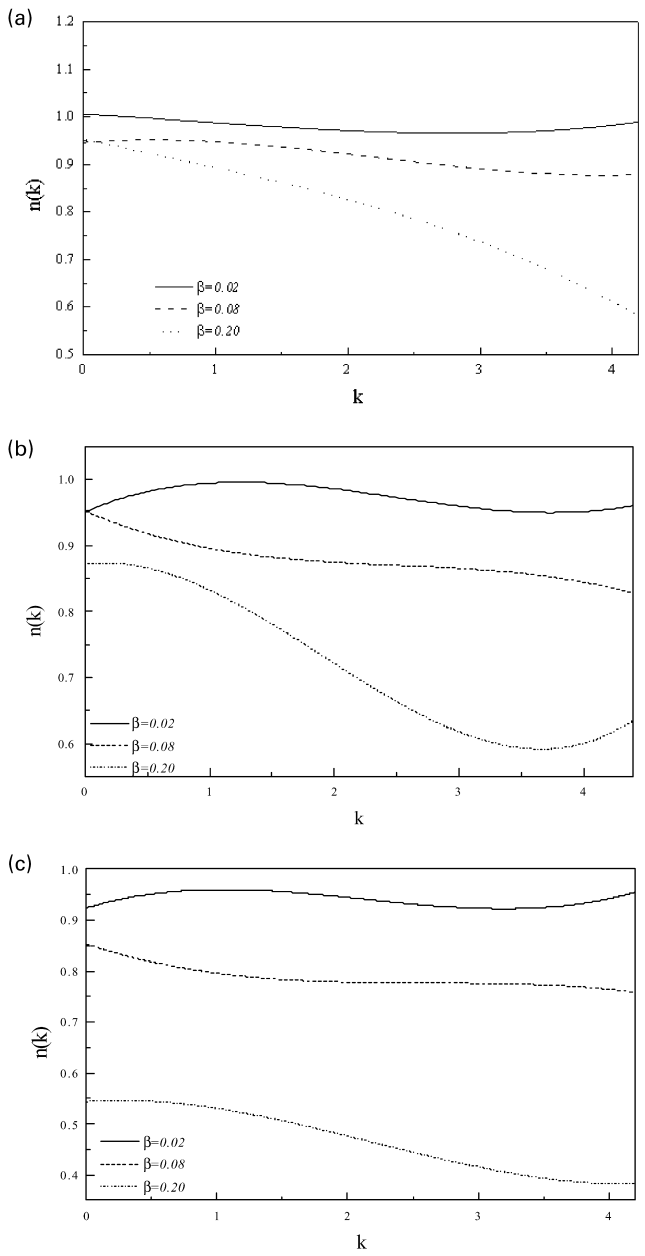

Fig. 6. (a) The variation of momentum distribution versus wave vector for different values of β ($\beta = 0.02, 0.08, 0.20$) for ($U = 6$, $E = 2$) (eV). (b) The variation of momentum distribution versus wave vector for different values of β ($\beta = 0.02, 0.08, 0.20$) for ($U = 6$, $E = 3$) (eV). (c) The variation of momentum distribution versus wave vector for different values of β ($\beta = 0.02, 0.08, 0.20$) for ($U = 6$, $E = 6$) (eV). (d) The variation of momentum distribution versus wave vector for ($U = 6$, $E = 2, 3, 6$ (eV) and $\beta = 0.02$.

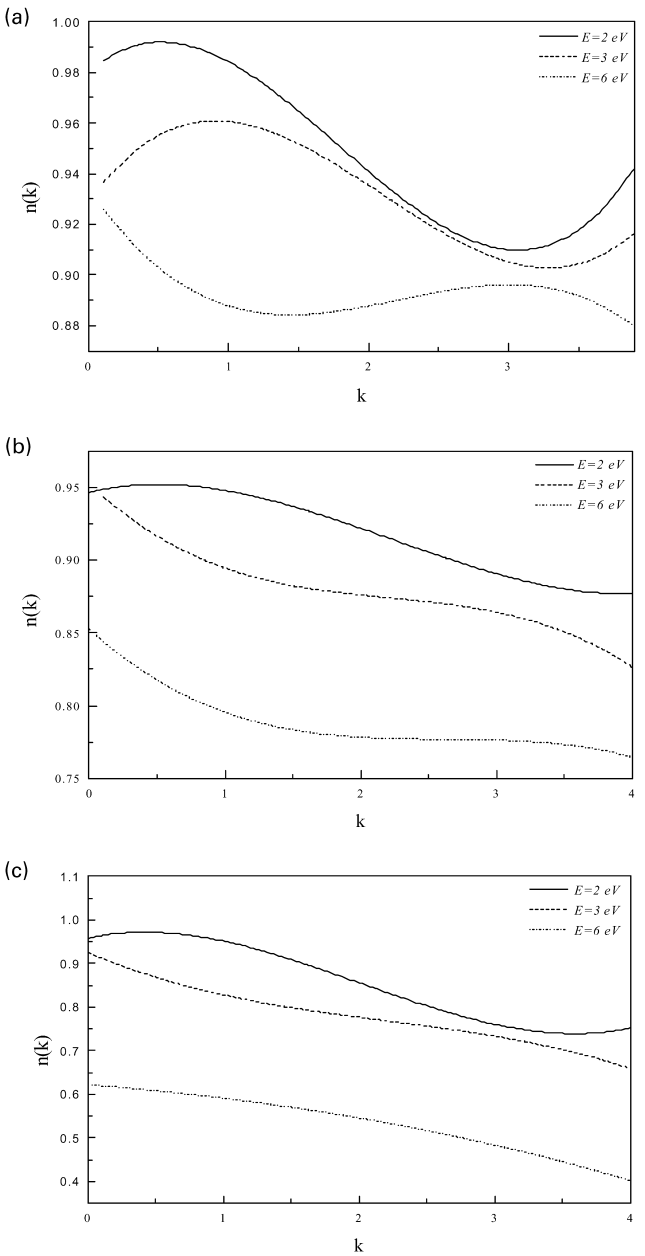

Fig. 7. (a) The variation of momentum distribution versus wave vector for ($U = 6$, $E = 2, 3, 6$) (eV) and $\beta = 0.04$. (b) The variation of momentum distribution versus wave vector for ($U = 6$, $E = 2, 3, 6$) (eV) and $\beta = 0.2$.

3.1.2. Intermediate coupling regime: $U \approx 4t$ and $E \approx U$, $E \approx U/2$, $EU/2$, $EU/2$)

Fig. 4(a)–(d) illustrates the size dependence of the momentum distribution for $U = 10$ eV and $E \approx 5, 8, 10$ and 13 eV, respectively. We notice that the behavior of $n(k)$ is typically the same for different values of β and (U, E). We draw also in Fig. 5(a)–(c), the effect of β ($\beta = 0.04, 0.08, 0.2$). In the intermediate coupling, the momentum distribution is less than the unity (as in the other regimes), confirming the effect of band filling [21,22].

3.1.3. Weakly coupling regime: $U4t$ and $E \approx U$, $E \approx U/2$, $EU/2$, $EU/2$)

To confirm our finding, we treat the weak coupling regime ($U < 4t$), given in Fig. 6(a)–(c), for $E \approx 2$, 3 and 6 eV, respectively, by investigating the effect of temperature β. We notice that the magnitude of $n(k)$ is approaching the unity and start decaying when E increases (see Fig. 7(a)–(c)) for ($\beta = 0.04, 0.08, 0.2$), respectively.

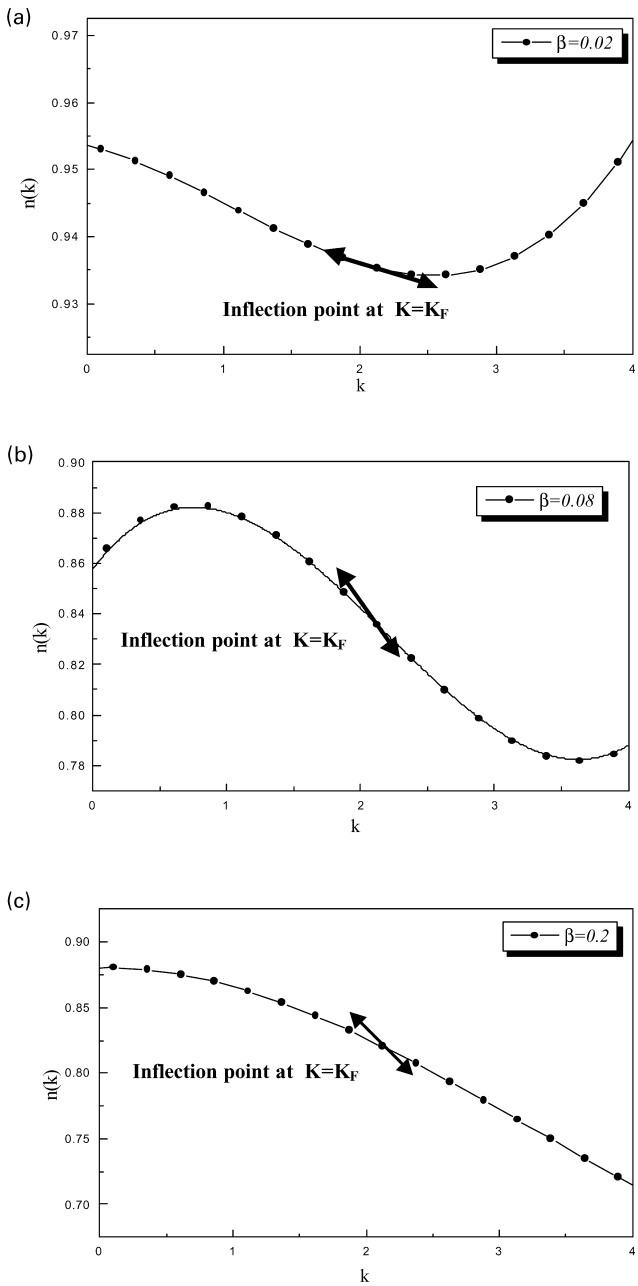

Fig. 8. (a)–(c) The exhibition of the inflection point in the variation of momentum distribution versus wave vector for $\beta = 0.04$, 0.08, and 0.2, respectively.

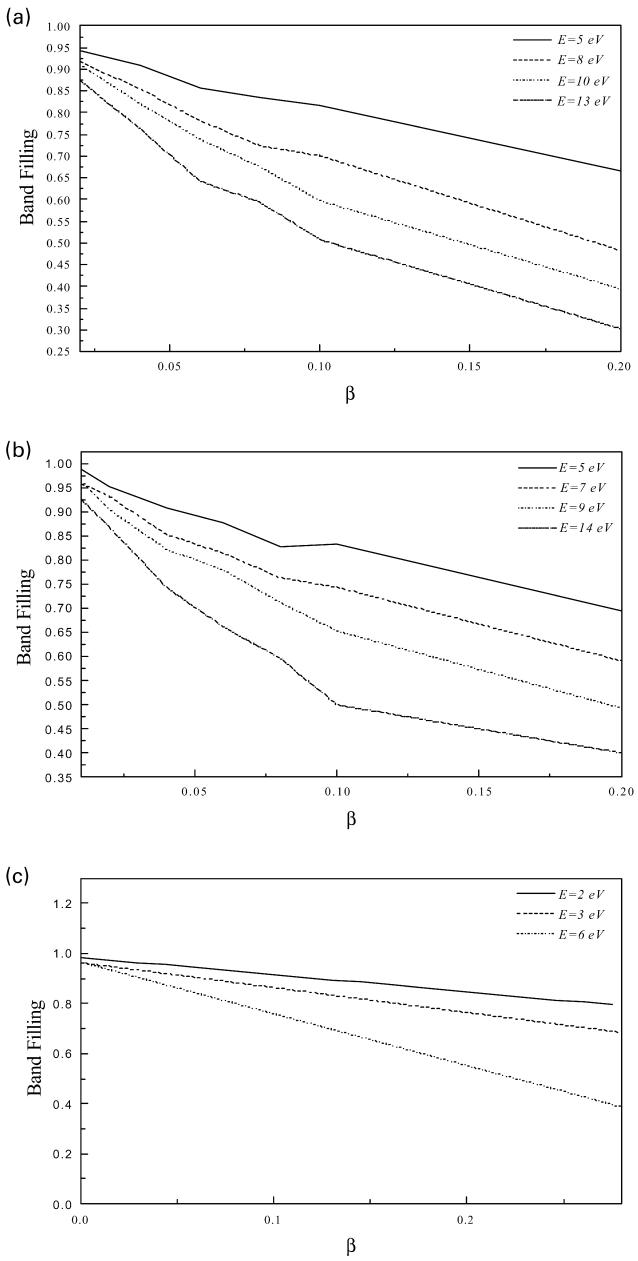

Fig. 9. Variation of the band-filling versus inverse temperature for: (a) $U = 14$, $E = 5$, 7, 9, 14 (eV); (b) $U = 10$, $E = 5$, 8, 10, 13 (eV); and (c) $U = 6$, $E = 2$, 3, 6 (eV).

As a general observation, there is a temperature-independent point at the free-electron value of the Fermi wave vector, for $k < k_F$ or $k > k_F$, $n(k)$ is approximately constant, but around k_F, $n(k)$ has a sudden change (an inflection point) which indicates a Fermi liquid behavior. We show this behavior, when we plot the results of Fig. 2(a) in separate curves, in Fig. 8(a)–(c), for $\beta = 0.04$, 0.08 and 0.2, respectively. These results agree fairly with Luttinger's theorem [23] and different results obtained from t/U expansion [7,22]. Note that the Luttinger's theorem does not hold since there is no jump in the momentum distribution (no Fermi surface). Nevertheless, $k = \pi/2$ remains an inflection point. Hence, the existence of an inflection point in the momentum distribution by itself cannot be taken as a proof for the existence of quasi-particles, but it is consistent with Sorella et al. [21,24–26] results, namely at half-filled, the numerical simulation are consistent with the absence of Fermi surface for relatively small system size (32×1 lattice in our case). This is also, due to the strong localization of electrons which occurs at half-filling case [21].

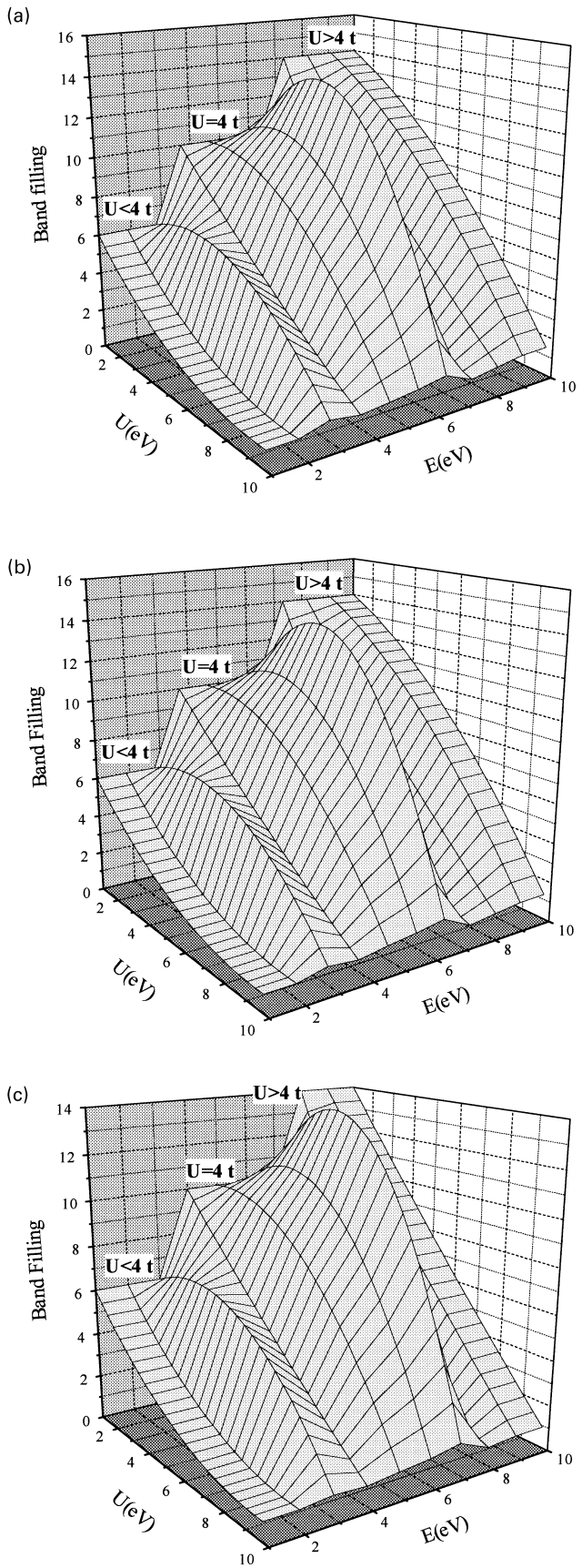

Fig. 10. (a)–(c) Variation of the band-filling (U, V) for $\beta = 0.02$, 0.08, 0.20, respectively.

3.2. Band filling

It is interesting to study the band filling in k-space, given by the following expression:

$$n = \frac{1}{2}\sum_{\sigma} n_{\sigma} \tag{13}$$

This observable confirms many results given by momentum distribution. The behavior of n for different values of inverse temperature and correlation parameters is shown in Fig. 9(a)–(c), from these graphs we see that the band filling is decreased as temperature is decreased and it's magnitude is always less than unity due to e–e interactions [1,22,24,25].

In Fig. 10(a)–(c), we show the variation of the band filling versus (U, E) for $(\beta = 0.04, 0.08, 0.2)$, respectively. The effect of localization is more significant, and the behavior of band filling is the same qualitatively but the magnitude of n is more influenced by correlation parameters, as (U, E) increase, the band filling is enhanced and this is clear from Eq. (13).

4. Conclusion

The electronic momentum distribution function is fundamental and gives more complementary information to other characterization to our understanding of quantum many-body systems in most area of physics. This observable, has been studied using different methods because clear differences between the Fermi liquid and the non-Fermi liquid (e.g. Luttinger liquid) behaviors can be found from $n(k)$.

Using the determinantal QMC approach and the so-called pseudo-fermionic field approximation, we calculate the electronic momentum distribution function $n(k)$ and show the electron–electron interactions effect. We have reported for different values of temperature and correlation parameters (U, E) the results of numerical simulation by Monte Carlo on the extended one-dimensional Hubbard by calculating $n(k)$ for different range coupling. Our results are in perfect agreement with the most current available results in *trans*-polyacetylene and different works in quasi-one-dimensional systems. Our calculation provides an alternative explanation to the Fermi liquid theory. Also, we have found an absence of the Fermi surface consistent with Luttinger's theorem. The calculation of the band filling observable for different correlation parameters (U, E) has confirmed the results given by the momentum distribution.

Acknowledgements

One of the authors (S. Goumri-Said) want to warmly thank Prof. E. Tossati and Prof. S. Baroni (University of

Sissa, Trieste, Italy), for numerous fruitful discussions during the Spring College on Numerical Methods in Electronic Structure Theory, the Abdus Salam International Centre for Theoretical Physics, Italy, 7–25 May 2001.

References

[1] Hubbard J. Proc R Soc (Lond) A 1963;276:238.
[2] Gutzwiller MC. Phys Rev Lett 1963;10:159.
[3] Soos ZG, Hennessy MH, Wen G. Chem Phys Lett 1997;274:189.
[4] Gebhard F. The Mott metal insulator transition. Berlin: Springer; 1997.
[5] Lieb EH. Phys Rev Lett 1989;62:1201.
[6] Lieb EH. Advances in dynamical systems and quantum physics. Singapore: World Scientific; 1995. p. 173.
[7] Takahashi M. J Phys C 1977;10:1928.
[8] Hirsch JE, Sugar RL, Scalapino DJ, Blankenbecler R. Phys Rev Lett 1981;47:1628.
[9] White SR, Scalapino DJ, Sugar RL, Loh EY, Gubernatis JE, Scalettar RT. Phys Rev B 1989;40:506.
[10] Hirsch JE, Sugar RL, Scalapino DJ, Blankenbecler R. Phys Rev B 1982;26:5033.
[11] Kim C, Matsura AY, Shen Z-X, Motoyama N, Eisaki H, Uchida S, Tohyama T, Maekawa S. Phys Rev Lett 1996;77:4054.
[12] Lieb EH, Wu FY. Phys Rev Lett 1968;20:1445.
[13] Trotter HF. Proc Am Math Soc 1959;10:545.
[14] Buendia GM. Phys Rev B 1986;33:3519.
[15] Hirsch JE. Phys Rev B 1983;28:4059.
[16] Hirsch JE. Phys Rev B 1985;31:4403.
[17] Schütt J, Schulte J, Böhm MC, Soos ZG. Mol Phys 1995;84:1127.
[18] Goumri-Said S, Moussa R, Dufour J-P, Salomon L, Aourag H. Physica B 2001;296:377.
[19] Yannoni CS, Clarke TC. Phys Rev Lett 1983;51:1191.
[20] Kivelson S, Heim D. Phys Rev B 1982;26:4278.
[21] Sorella S, Tosatti E, Baroni S, Car R, Parrinello M. Int J Mod Phys B 1988;1:993.
[22] Bourbonnais C, Nélisse H, Reid A, Tremblay A-MS. Phys Rev B 1989;40:2297.
[23] Luttinger JM. Phys Rev 1982;121:942.
[24] Sorella S, Baroni S, Car R, Parrinello M. Eur Phys Lett 1989;8:663.
[25] Sorella S, Baroni S, Car R, Parrinello M. Eur Phys Lett 1990;12:721.
[26] Parola A, Sorella S. Phys Rev Lett 1990;64:1831.